RSC Advances

PAPER

View Article Online
View Journal | View Issue

Cite this: *RSC Adv.*, 2019, **9**, 14242

Selective oxidation of 5-hydroxymethylfurfural into 2,5-diformylfuran over VPO catalysts under atmospheric pressure†

Jinhua Lai, ‡[a] Kai Liu,‡[a] Shuolin Zhou, [ab] Du Zhang,[a] Xianxiang Liu, *[a] Qiong Xu[a] and Dulin Yin[a]

Received 22nd March 2019
Accepted 2nd May 2019

DOI: 10.1039/c9ra02213a

rsc.li/rsc-advances

Vanadium phosphate oxide (VPO) heterogeneous catalysts with different V/P molar ratios were prepared and used for selective oxidation of biomass-derived 5-hydroxymethylfurfural (HMF) to produce 2,5-diformylfuran (DFF) in the liquid phase. It was found that the VPO catalyst with V/P molar ratio 0.25 exhibited the best catalytic performance. Then the VPO catalyst was utilized to catalyze the oxidation of HMF in a batch reactor under different conditions, in terms of type of solvent (water and organic), reaction time and temperature. A high DFF yield of 83.6% with HMF conversion of 100% was obtained under atmospheric pressure.

Introduction

In recent years, the high value-added chemicals and fuels prepared from renewable natural biomass resources have captured intense interest, coined "biorefinery".[1–3] Among them, the dehydration of C6 based carbohydrates can generate an important platform chemical 5-hydroxymethylfurfural (HMF), which is considered to be one of the top value-added chemicals. 2,5-Diformylfuran (DFF) is one of the main products of HMF oxidation, and has been used as a starting material for the synthesis of ligands, drugs, pesticide antifungal agents, fluorescent materials and new polymeric materials.[4,5]

However, as shown in Scheme 1, the HMF structure contains a hydroxyl and a formyl moiety together with a furan ring, opening an avenue for chemical reactions. Therefore, the oxidation of HMF makes it susceptible to undergo many side reactions such as over oxidation of DFF into 2,5-furandicarboxylic acid (FDCA), the oxidation of aldehyde to 5-hydroxymethyl-2-furancarboxylic acid (HMFCA), decarbonylation, and cross-polymerization to produce unwanted byproducts. Therefore, it is still a challenge to selectively oxidize HMF into DFF.

How to achieve selective oxidation of HMF to prepare DFF under mild conditions, it has always been an important and challenging subject. To date, there are plenty of catalysts employed in selective oxidation of HMF into DFF, such as the manganese oxide-based material,[6–8] GO-related materials,[9] supported Ru catalysts[10–12] and vanadium-based catalysts.[13–16] Zhang *et al.*[17–19] have been committed to research in this area and developed a series of catalysts with excellent catalytic activity. Due to the high price of noble metal, developing cheap transition metal-based heterogeneous catalysts for the synthesis of DFF from the selective oxidation of HMF is thus highly desirable. Among these catalysts, vanadium-containing catalysts are noticeable. In the past decade, some methods on the aerobic oxidation of alcohols using relatively cheap V based catalysts were reported. Inspired by the excellent catalytic activity of VPO catalysts in the oxidation of alcohols, herein, we prepared a series of VPO catalysts with different V/P molar ratios by using the liquid phase method, and used as a novel heterogeneous catalyst for the selective oxidation of HMF into DFF.

Experimental

Materials

5-Hydroxymethylfurfural (99.5%) and 2,5-diformylfuran were purchased from Sinopharm Chemical Reagent Co., Ltd.

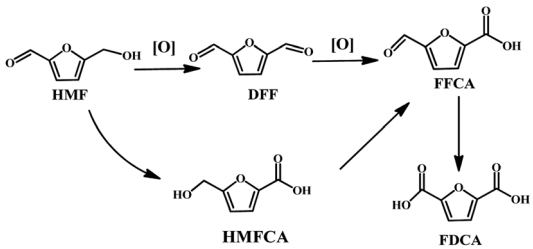

Scheme 1 Possible oxidation products from the oxidation of HMF.

[a]*National & Local Joint Engineering Laboratory for New Petro-chemical Materials and Fine Utilization of Resources, Key Laboratory of the Assembly and Application of Organic Functional Molecules of Hunan Province, College of Chemistry and Chemical Engineering, Hunan Normal University, Changsha 410081, PR China. E-mail: lxx@hunnu.edu.cn; Fax: +86 731 88872531; Tel: +86 731 88872576*

[b]*Junior Education Department, Changsha Normal University, Changsha 410100, PR China*

† Electronic supplementary information (ESI) available. See DOI: 10.1039/c9ra02213a

‡ These authors contributed equally.

(Shanghai, China). NH_4VO_3 and H_3PO_4 were purchased from Sinopharm Chemical Reagent Co., Ltd (Shanghai China). All the chemicals were of analytical grade and used without further purification. Ultrapure water was used for the catalyst preparation and catalytic reactions.

Preparation of catalyst

Vanadium phosphate oxide (VPO) was prepared according to the following procedure. V_2O_5 (1.4 g), derived from the pyrolysis of NH_4VO_3 at 180 °C, and H_3PO_4 (85%, 7 g) were refluxed in isobutanol (25 mL) at 120 °C for 12 h. The resulting solid was isolated by vacuum filtration, washed with isobutanol, and dried under vacuum at 80 °C. Powder X-ray pattern of the solid prasinous product corresponded to that found for $VO(H_2PO_4)_2$.

Synthesis of DFF from HMF

The oxidation of HMF in the air under atmospheric pressure was performed in a 25 mL round bottom flask, which was coupled with a reflux condenser using the following general procedure. Typically, HMF (0.1 mmol, 12.6 mg) was firstly dissolved into DMSO (5 mL) in the flask with a magnetic stirrer. Then, 10 mg VPO catalysts were added into the reaction mixture. The mixture was heated to the desired temperature while stirring under an air atmosphere. After reaction, the reaction solution was quantitatively analyzed by HPLC. According to test results, the oxidation of HMF mainly leads to DFF, HMFCA, 5-formyl-2-furancarboxylic (FFCA) and FDCA.

Quantification of the products

The product analysis was performed using Agilent 1100 HPLC system equipped with Agela Technologies Venusil XBP C18(L) (4.6 × 250 mm) and a UV-Vis (280 nm) detector. The mobile phase was constituted of acetonitrile and 0.1 wt% acetic acid aqueous solution (v : v = 15 : 85), and the samples was eluted at a rate of 0.5 mL min^{-1} at 30 °C. The amount of each compound was quantified by external standard calibration curve method.

To calculate HMF conversion, DFF selectivity and yield are defined as follow:

$$\text{HMF conversion} = (1 - \text{moles of HMF/moles of HMF added}) \times 100\%$$

$$\text{DFF selectivity} = \text{moles of DFF/(moles of HMF added} - \text{moles of HMF)} \times 100\%$$

$$\text{DFF yield} = \text{moles of DFF/moles of HMF added} \times 100\%$$

Results and discussion

Catalyst characterization

The VPO catalyst was characterized using XRD, TEM, TG-DTG, Raman and FI-IR analysis. The XRD pattern in Fig. 1 illustrated the $VO(H_2PO_4)_2$ crystal structure with JCPDS card 40-0038 for the VPO catalyst, demonstrating that this phase has been successfully synthesized. However, the VPO catalyst demonstrated the largely enhance (002) and (121) facet signal at 22.38° and 24.96°.

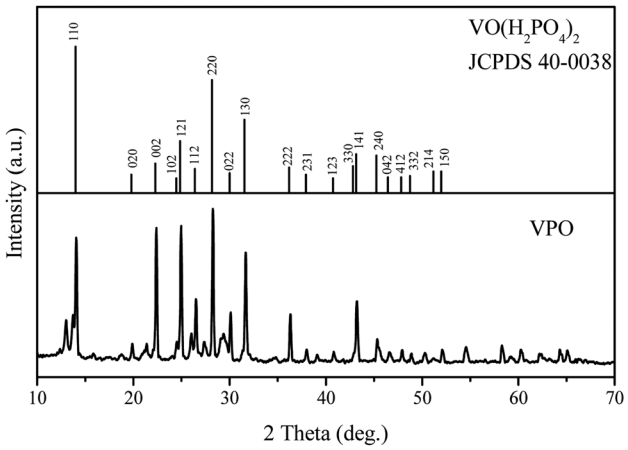

Fig. 1 XRD patterns of VPO.

Fig. 2 showed TEM images of VPO catalyst at different magnifications. The TEM observation in Fig. 2a verified a nanosheet structure of VPO covered by a different phase (Fig. 2b). This new phase seems to be a film forming some aggregates or clusters (Fig. 2c and d) on the nanosheets. From the Fig. 2, it can be clearly distinguished the aggregates with multiple grains of different sizes. In agreement with XRD, this dispersed phase seems to be a mixture of VPO mixed-oxide species.[20,21]

The thermogravimetric analysis for VPO sample carried out in nitrogen flow. It can be seen from the Fig. 3 that the VPO catalyst has three weight loss stages. Firstly, around 5% of mass loss at temperatures lower than 150 °C, due to the loss of absorbed water; second, the mass loss lower than 5% at temperatures range at 150–250 °C, due to the loss of crystal water; then, a flat region up to 300 °C; and then it starts to be decomposed into $VO(PO_3)_2$.[22] Thus, this catalyst can be used under oxidizing conditions up to 300 °C. As expected, the VPO catalyst profile only presents a mass loss at low temperature

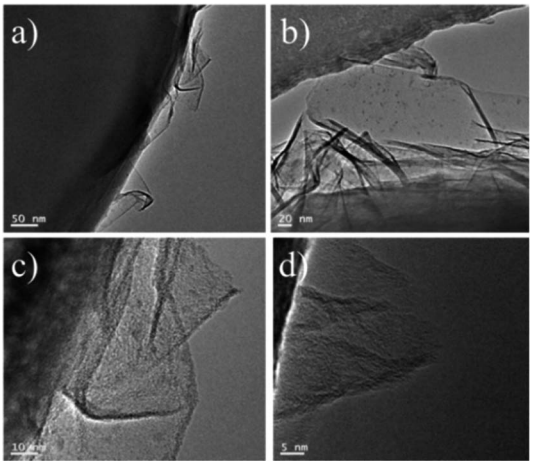

Fig. 2 TEM images of VPO catalysts.

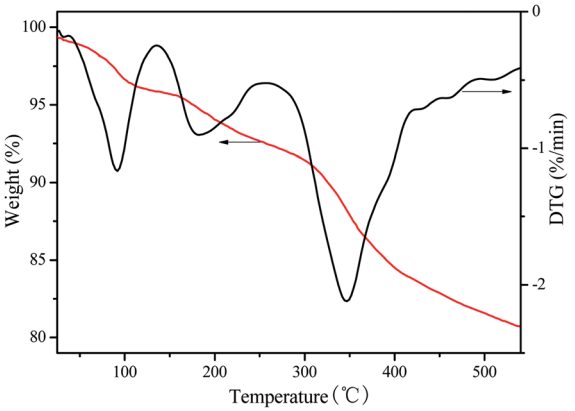

Fig. 3 TG-DTG curves of VPO.

due to absorbed water and then it does not present a weight loss when the temperature increased.

The FT-IR spectra of different V_2O_5 and a series of the VPO catalyst with different V/P molar ratios were analyzed (Fig. 4). The FT-IR spectra of different V_2O_5 illustrated the typical V_2O_5 crystal structure for both the commercial bulk V_2O_5 and the V_2O_5 derived from the pyrolysis of NH_4VO_3. However, the V=O of the V_2O_5, derived from the pyrolysis of NH_4VO_3, demonstrated the smaller wave number (below 1000 cm^{-1}). And the adsorption peaks appearing at around 3200 cm^{-1} and 1400 cm^{-1} correspond to the N–H. For four curve of VPO, with the increase of V_2O_5 content in VPO, the characteristic absorption intensity of V=O (below 1000 cm^{-1}) increases continuously, and the vibration absorption intensity of two PO_3 groups (1000–1300 cm^{-1}) decreases, which differ by the type of symmetry.[23] The broad peaks around 3600 cm^{-1} and 1640 cm^{-1} are attributed to the stretching and bending modes of the O–H of surface hydroxyl groups and physically adsorbed water. The peak at 3420 cm^{-1} arises from the O–H stretching vibration of V–O–H.

The Raman spectra of different V_2O_5 samples in Fig. 5 illustrated the V_2O_5 crystal structure. However, the V_2O_5 derived from the pyrolysis of NH_4VO_3 gave a new intense Raman band at 964 cm^{-1} compared with the commercial bulk

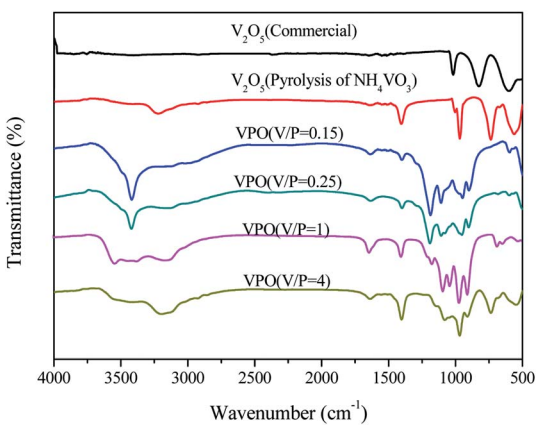

Fig. 4 FT-IR spectra of different V_2O_5 and a series of the VPO catalysts with different V/P molar ratios.

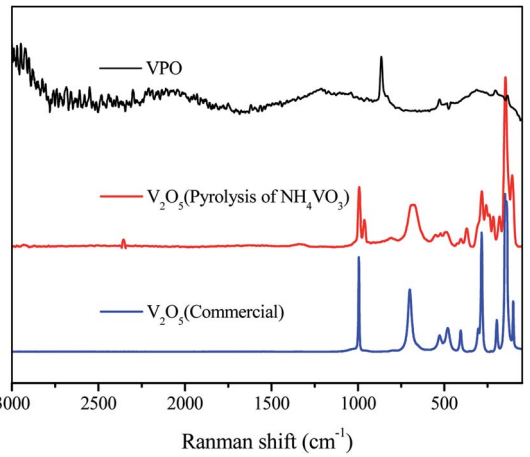

Fig. 5 Raman spectra of VPO and different V_2O_5.

V_2O_5. In agreement with FT-IR, it is characteristic of V–OH. There is no V_2O_5 Raman bands in Raman spectrum of VPO, and Raman bands near 1034 cm^{-1} redshifts upon hydration and it is characteristic of the V=O bond stretching mode,[24,25] confirming the presence of dispersed vanadium oxide species (VO_X) and well dispersed. The intense Raman band at 940 cm^{-1} has been assigned to $VO(H_2PO_4)_2$,[26] same as XRD and FT-IR result. Thus, the $VO(H_2PO_4)_2$ is certainly achieved.

Effect of V/P molar ratios on the selective oxidation of HMF

The catalytic activity of the as-prepared VPO catalysts with different V/P molar ratios was evaluated by the oxidation of HMF in DMSO under atmospheric air pressure at 120 °C. Fig. 6 depicted the results of HMF conversion and products selectivity using various VPO catalysts. HMF conversion and selectivity of DFF were all changed greatly with the increase of vanadium content in the VPO catalysts. When V/P molar ratio of the VPO catalyst was 4, the HMF was fully transformed, but the selectivity and yield of the DFF were relatively low. This implies an increase in the V/P ratio can maintain the oxidation properties of VPO catalyst and increases in turn the formation of side products, the lower DFF selectivity accordingly.[27,28] In addition,

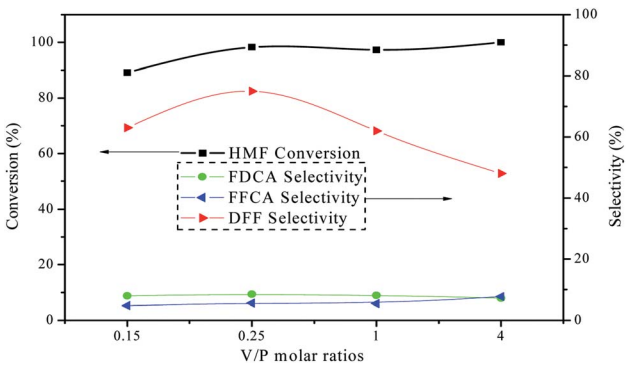

Fig. 6 The results of HMF oxidation over the VPO catalysts with different V/P molar ratios under atmospheric pressure. Reaction conditions: 0.1 mmol HMF, 10 mg catalyst, 5 mL DMSO, 120 °C, 10 h, in the air.

V_2O_5 was also active for HMF oxidation with conversion of 89.5% under the same reaction conditions, yet with the lower selectivity toward DFF of 69.7%, since further oxidation to form FFCA (10.2%) and FDCA (9.9%) easily occurred. While the VPO catalyst with V/P molar ratio 0.25, HMF was almost quantitatively converted, and the selectivity of DFF reached the maximum 75.0%. This enlightens that the VPO catalyst exhibits excellent catalytic activity at room pressure, compared to 5% conversion in the previous work.[29] Therefore, all subsequent experiments used of the VPO catalyst with V/P molar ratio 0.25.

Effect of solvents on the selective oxidation of HMF

The selective oxidation of HMF was further carried out in a variety of solvents. As shown in Table 1, the solvent showed a remarkable effect on the oxidation of HMF. DMSO with high polarity and high boiling point was found to be the best solvent. HMF completely converted and the selectivity of DFF reached 83.6% when using DMSO as the solvent (Table 1 Entry 5). Moderate HMF conversions around 30–40% were obtained in MIBK and DMF, as much more DFF was further oxidized into FDCA. The selectivity of DFF in DMF was the lowest of all testing organic solvent. Reaction carried in toluene and water produced low HMF conversion (Table 1 Entry 1 and Entry 2). Yang *et al.*[30] also reported that polar solvent like DMSO shows better HMF conversion and DFF selectivity as compared to non-polar solvent such as toluene. Hence, further study was done by taking DMSO as solvent for the selective oxidation of HMF into DFF.

Effect of time on the selective oxidation of HMF

Fig. 7 showed time course for each product in the VPO-catalyzed oxidation of HMF to DFF. As shown in Fig. 7, the oxidation of HMF was very fast, and then slowed down. The fast reaction rate in the initial stage should be due to the high concentration of HMF at an early reaction stage.[31] HMF was fully converted after 10 h, and DFF was obtained in a highest yield of 83.2%. FDCA was obtained in a highest yield of 12.0% at 2 h, and the yield of FFCA increased slowly and reached 5.4%. HMFCA was not detected during this reaction. It is therefore expected that HMF is oxidized into DFF, and that FDCA formed though FFCA derived from DFF.

Table 1 Effect of solvents on the selective oxidation of HMF into DFF[a]

Entry	Solvent	HMF conversion (%)	Selectivity (%)			DFF yield (%)
			FDCA	FFCA	DFF	
1	H_2O	22.0	—	—	—	—
2	Toluene	15.0	—	—	100	15.0
3	MIBK	43.1	28.9	25.8	45.2	19.5
4	DMF	30.5	27.4	—	37.1	11.3
5	DMSO	100	9.2	6.1	83.6	83.6

[a] Reaction condition: 0.1 mmol HMF, 10 mg VPO, 5 mL solvent, 120 °C, 10 h, in the air.

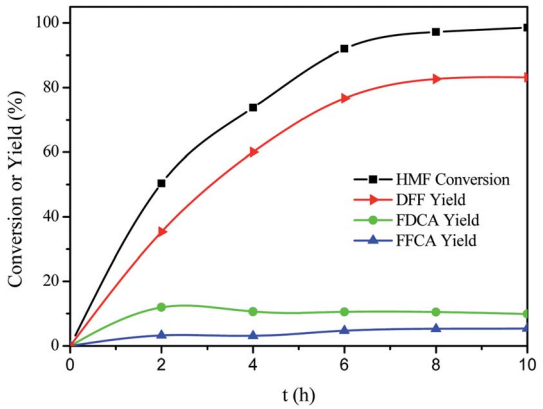

Fig. 7 Time courses of HMF oxidation over the VPO catalysts under atmospheric pressure. Reaction conditions: 0.15 mmol HMF, 10 mg VPO, 10 mL DMSO, 120 °C, in the air.

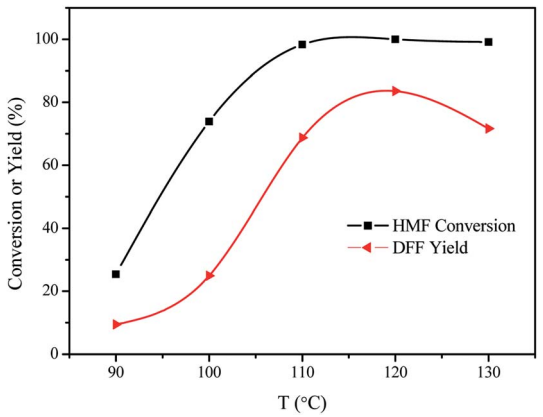

Fig. 8 The results of HMF oxidation over the VPO catalysts at different reaction temperatures under atmospheric pressure. Reaction conditions: 0.1 mmol HMF, 10 mg VPO, 5 mL DMSO, 10 h, in the air.

Effect of reaction temperature on the selective oxidation of HMF

The effect of the reaction temperature was also studied and the results are shown in Fig. 8. HMF conversion and DFF yield increased with the increase of reaction temperature between 90 °C and 110 °C. HMF conversion was obtained in 25.4% when the reaction was carried out at the reaction temperature of 90 °C. Furthering increasing the reaction temperature to 110 °C, HMF conversion increased to 98.3% after 10 h. These results indicated that high reaction temperature promoted the selective oxidation of HMF into DFF. Quantitative HMF conversion was reached when the reaction was carried out at 120 °C and 130 °C. As far as the products yield, the yield of DFF was also greatly affected by the reaction temperature. The yield of DFF gradually increased with the increase of the reaction temperature. The highest yield of DFF was obtained in 83.6% at 120 °C and it slightly decreased to 71.7% at 130 °C.

Conclusions

In conclusion, a new and environmentally friendly method was developed for the synthesis of DFF from the selective oxidation of HMF into DFF. The prepared VPO catalysts showed an excellent catalytic performance with DFF yield of 83.6% and high HMF conversion of 100% under atmospheric pressure in the air. Several important parameters were studied for the oxidation of HMF into DFF. It was found that the solvents played a crucial role in the conversion of HMF and the selectivity of DFF. This work opens up a new way to apply VPO as heterogeneous catalyst in the sustainable conversion of biomass derived compounds into valuable chemicals.

Conflicts of interest

There are no conflicts to declare.

Acknowledgements

The authors gratefully acknowledge the financial support of the National Natural Science Foundation of China (21606082 and 21776068), Hunan Provincial Natural Science Foundation of China (2018JJ3334), the Scientific Research Fund of Hunan Provincial Education Department (17C0951) and Hunan Provincial Innovation Foundation for Postgraduate (CX2018B295).

Notes and references

1 B. You, X. Liu, N. Jiang and Y. Sun, *J. Am. Chem. Soc.*, 2016, **138**, 13639–13646.
2 M. Besson, P. Gallezot and C. Pinel, *Chem. Rev.*, 2014, **114**, 1827–1870.
3 J. C. Colmenares and R. Luque, *Chem. Soc. Rev.*, 2014, **43**, 765–778.
4 X. X. Liu, J. F. Xiao, H. Ding, W. Z. Zhong, Q. Xu, S. P. Su and D. L. Yin, *Chem. Eng. J.*, 2016, **283**, 1315–1321.
5 B. Liu and Z. Zhang, *ChemSusChem*, 2016, **9**, 2015–2036.
6 L. Chen, W. Yang, Z. Gui, S. Saravanamurugan, A. Riisager, W. Cao and Z. Qi, *Catal. Today*, 2019, **319**, 105–112.
7 B. Liu, Z. Zhang, K. Lv, K. Deng and H. Duan, *Appl. Catal., A*, 2014, **472**, 64–71.
8 X. Tong, L. Yu, H. Chen, X. Zhuang, S. Liao and H. Cui, *Catal. Commun.*, 2017, **90**, 91–94.
9 G. Lv, H. Wang, Y. Yang, T. Deng, C. Chen, Y. Zhu and X. Hou, *ACS Catal.*, 2015, **5**, 5636–5646.
10 C. A. Antonyraj, J. Jeong, B. Kim, S. Shin, S. Kim, K. Y. Lee and K. C. Jin, *Ind. Eng. Chem.*, 2013, **19**, 1056–1059.
11 J. Nie, J. Xie and H. Liu, *J. Catal.*, 2013, **301**, 83–91.
12 A. Takagaki, M. Takahashi, S. Nishimura and K. Ebitani, *ACS Catal.*, 2011, **1**, 1562–1565.
13 Y. Yan, K. Li, J. Zhao, W. Cai, Y. Yang and J.-M. Lee, *Appl. Catal., B*, 2017, **207**, 358–365.
14 C. A. Antonyraj, B. Kim, Y. Kim, S. Shin, K. Y. Lee, I. Kim and K. C. Jin, *Catal. Commun.*, 2014, **57**, 64–68.
15 N. T. Le, P. Lakshmanan, K. Cho, Y. Han and H. Kim, *Appl. Catal., A*, 2013, **464–465**, 305–312.
16 X. Jia, J. Ma, M. Wang, Z. Du, F. Lu, F. Wang and J. Xu, *Appl. Catal., A*, 2014, **482**, 231–236.
17 Y. Ren, Z. Yuan, K. Lv, J. Sun, Z. Zhang and Q. Chi, *Green Chem.*, 2018, **20**, 4946–4956.
18 B. Liu, Y. Ren and Z. Zhang, *Green Chem.*, 2015, **17**, 1610–1617.
19 Z. Yuan, B. Liu, P. Zhou, Z. Zhang and Q. Chi, *Catal. Sci. Technol.*, 2018, **8**, 4430–4439.
20 R. Berenguer, J. Fornells, F. J. García-Mateos, M. O. Guerrero-Pérez, J. Rodríguez-Mirasol and T. Cordero, *Catal. Today*, 2016, **277**, 266–273.
21 D. B. Williams and C. B. Carter, *Transmission Electron Microscopy. Part 2: Diffraction*, Springer, New York, 2nd ed., 2009, pp. 293–295.
22 V. Caignaert, M. S. Kishore, V. Pralong, B. Raveau, N. Creon and H. Fjellvaag, *J. Solid State Chem.*, 2007, **180**, 2437–2442.
23 Y. H. Taufiq-Yap and C. K. Goh, *Pertanika J. Sci. Technol.*, 2003, **11**, 293–300.
24 M. A. Bañares and I. E. Wachs, *J. Raman Spectrosc.*, 2002, **33**, 359–380.
25 I. E. Wachs, J. M. Jehng, G. Deo, B. M. Weckhuysen, V. V. Guliants, J. B. Benziger and S. Sundaresan, *J. Catal.*, 1997, **170**, 75–88.
26 F. B. Abdelouahab, R. Olier, N. Guilhaume, F. Lefebvre and J. C. Volta, *J. Catal.*, 1992, **134**, 151–167.
27 A. Datta, S. Sakthivel, M. Kaur, A. M. Venezia, G. Pantaleo and A. Longo, *Microporous Mesoporous Mater.*, 2010, **128**, 213–222.
28 F. L. Grasset, B. Katryniok, S. Paul, V. Nardello-Rataj, M. Pera-Titus, J. M. Clacens, F. De Campo and F. Dumeignil, *RSC Adv.*, 2013, **3**, 9942–9948.
29 C. Carlini, P. Patrono, A. M. R. Galletti, G. Sbrana and V. Zima, *Appl. Catal., A*, 2005, **289**, 197–204.
30 Z. Z. Yang, J. Deng, T. Pan, Q. X. Guo and Y. Fu, *Green Chem.*, 2012, **14**, 2986–2989.
31 G. D. Yadav and R. V. Sharma, *Appl. Catal., B*, 2014, **147**, 293–301.

